TREND

Trapped Radiation Environment Model Development

Evaluation of the INP Radiation Belts Models

Technical Note A

ESTEC/Contract No. 9828/92/NL/FM[1]

A. Beliaev (MSU)
J. Lemaire (IASB)

June 12, 1994

[1]ESA Technical Management: E.J. Daly (WMA)

Contents

List of Figures

List of Tables

Introduction

This document contains the Technical Note A for the study which has been carried out according to Work Package WP 2.1 of the TREND-2 Rider (contract 9828/92/NL/FM).

1 Purpose

The objective of WP 2.1 is to evaluate models of the Earth's radiation belts, which were developed at the Institute of Nuclear Physics, Moscow State University (INP MSU), and to compare them with the AP-8 and AE-8 models developed by NASA.

This study should be useful to all those scientists and engineers who use empirical models for evaluation of fluences and radiation doses for specific space missions within the Earth's radiation environment.

2 Scope

The goal of the proposed work is to compare the models of trapped radiation particles fluxes in the magnetosphere, developed by INP MSU (hereafter called the 'INP models') with the AP-8 and AE-8 models developed by NASA.

Such a comparison implies:

1. Comparison of the methods used in both of these models, such as:
   - definition of the coordinate systems used (B, L);
   - methods used for data storage in the databases and the possible influence of the storage method on the precision of the model;
   - methods used to interpolate between the data set grid nodes and the consequences on the interpolated flux values.
2. Comparison of the model limits, such as:
   - regions of B, L space and energies covered by model data sets;

- regions of space coordinates where the values of the fluxes are significant, i.e. above threshold;

3. Comparison of the equatorial electron and proton fluxes for both sets of models, including:
   - comparing values of fluxes;
   - comparing the influence of solar activity on the models i.e. the difference between fluxes for years of solar maximum and solar minimum.
4. Comparison of the distribution of the particle fluxes along magnetic field lines and for constant L-values using different magnetic field models.
5. Comparison of the results of fluence calculations for different satellite orbits.

3 Definitions, acronyms and abbreviations

IASB/BIRA - Institute of Space Aeronomy, Brussel, Belgium

INP - Institute of Nuclear Physics

LEO - Low-Earth Orbit

MSU - Moscow State University

NASA - National Aeronautics and Space Administration

NSSDC - National Space Science Data Center

4 Overview

In Chapter 1 the physical description of NASA and INP trapped radiation models is given. In Chapter 2 the structure of database defining the model and the interpolation algorithms of both sets of models are described. In Chapter 3 flux values as well as fluences deduced from the NASA and the INP models are compared.

Chapter 1

General Description

Empirical models consist of files, containing flux values at grid points, interpolation method, providing the mean for the calculating of model values at arbitrary points and user interface to communicate with the model. Below we'll describe briefly these parts both for NASA trapped radiation models and INP models.

1 Description of NASA trapped radiation models

Several models of trapped radiation environment were published by NASA during the period of 1964-1991 (Vette 1991b). The latest in the set of NASA models, AP-8 for protons and AE-8 for electrons are described by Sawyer and Vette (1976) and Vette (1991a).

Both AE-8 and AP-8 models are static representation of trapped radiation environment, with local time dependence averaged out. There are four models, conventionally named AP-8MIN, AP-8MAX, AE-8MIN, AE-8MAX. They correspond to conditions of solar minimum and maximum.

The models use the $B/B_0, L$ coordinate system to describe location in space. L is McIlwain's parameter (McIlwain 1961) which plays the role of radial coordinate; in the case of a pure dipole magnetic field L corresponds to the radial distance at which a magnetic field line crosses the geomagnetic equator, i.e. where B_0 is the field intensity. B/B_0 is used to locate the position along the field line and is defined as the ratio of magnetic field strength in this point to B_0, the minimal value of magnetic field strength along the given field line. The values of B/B_0 change from 1 (which corresponds to magnetic equator in pure dipole magnetic field) to some maximum value, B_c which normally corresponds to the point of *atmospheric cutoff*, where particles are absorbed by the dense atmosphere.

For series of discrete values of L the model provides the values the logarithm

of equatorial flux, followed by scaled increments in B/B_0 required to produce fixed decrements in the logarithm of flux. All this is then repeated for a series of particle energies E covering the whole energy spectrum of the trapped electron and protons.

Special subroutines TRARA1 and TRARA2 are included in the model. They are used to perform interpolation in $E, L, B/B_0$ space. It should be noted, that interpolation problems with these subroutines were reported by Daly and Evans (1993). Instead of B/B_0 they suggested to use for linear interpolation new coordinate ϕ defined as

$$\phi = \arcsin \frac{B - B_0}{B_c - B_0}$$

This linear interpolation in E, L, ϕ space is done with a new subroutine TRARAP. Daly and Evans (1993) have shown that the ripples, usually obtained in fluxes contour lines with TRARA1 and TRARA2 subroutines, dissapear almost completely with TRARAP.

Due to the fact that original AP-8 datasets for solar minimum were too large to fit in the memory of computers commonly used at the epoch so called"compressed" version of AP-8 models was produced by NSSDC. The "compressed" versions of AP-8 models are described in a letter of the NSSDC Director to the users of NASA model (see Vette (1977)).

To model the time variations of flux value in the outer part of the electrons radiation belt, the statistical standard deviation of electrons flux value was introduced in AE-8. It is defined in the whole energy range of the model and for $3 < L < 11$ as tabulated function, given in Vette (1991a). This tabulated function gives the standard deviation of the logarithmmic flux as function of L and E.

Some parameters of AP-8/AE-8 models are presented in the Table 1, which is compiled from (Vette 1991b) and (Gaffey & Bilitza 1994).

Table 1. Characteristics of NASA trapped radiation models

Characteristic	AP-8	AE-8
Energy Range (MeV)	0.1–400	0.04–7
L range	1.15–6.6	1.2–11
Epoch	1964/1970	1964/1970
Date of Publication	1976	1983 (documented in 1991)
Number of Satellites	24	24
Number of Instruments	29	26
Number of Data Channels used	101	95
Channel-Months of Data	264	1303

NSSDC distributes also a FORTRAN interactive program named DRIVER which

uses subroutines `TRARA1` and `TRARA2` to retrieve the fluxes at given point of $E, L, B/B_0$.

2 Description of INP trapped radiation models

Since the 1970s, the Institute of Nuclear Physics (INP), Moscow State University is developing various models of the space environment. The first trapped radiation belts models developed at INP was published in Cosmos Model-82 (1983). The most recent models is described by Getselev et al. (1991). These models will be called INP models later in this document.

The NASA models were used as base models to produce reference spectra to which more recent satellite observations were then compared to those reference spectra. The data, collected with the spacecraft such as ISEE-1 (Williams & Frank 1984) (experiment PI - D.J. Williams, experiment data available from NSSDC), SCATHA (Davidson et al. 1988), GORISONT (Grafodatsky et al. 1989), COSMOS-900 (Goriainov et al 1983, Vlasova et al. 1984), INTERCOSMOS-19 (Volkov et al. 1985). Theoretical considerations based on low altitudes satellite data (Savun & Yushkov 1985) have been used to update the flux values in limited region of E, L, B space.

Some earlier versions of these models have been adopted as USSR State Standards (GOST 1986).

The INP models are static representation of trapped radiation particles flux, with local time dependencies averaged out like AE-8/AP-8 models. There are four models, two for protons and two for electrons, one for solar minimum and one for solar maximum. In the rest of the document, they will be named INP-PROTMIN, INP-PROTMAX, INP-ELECMIN, INP-ELECMAX. These names correspond to data file names.

Unlike the NASA models, INP models uses the B, L coordinate system to identify a drift shell. In the NASA models B/B_0 is used instead of B. For each L value, equatorial flux values and a number of off equator flux values are provided for the series of energies and for a set of tabulated values of B. The magnetic field models used to calculate B and L are assumed to be the same, i.e.: the Jensen and Cain (1960) model or GSFC12/66 model, updated to 1970 (Heynderickx et al. 1994).

Chapter 2

Comparison of model structure and organisation

1 Introduction

Both sets of models are organised as a three-dimensional matrix in E, L, B (or $E, L, B/B_0$) space. However, there are differences in the coordinate system chosen to store the values and to interpolate between grid points. These differences will be described below. One major difference is that in the INP models the coordinate B has not been replaced by B/B_0 as in the NASA models.

2 Models Ranges and Limits

The ranges and limits of AE-8/AP-8 and INP models are briefly summarised in Table 2.

The computer programs originally provided with the models, issue warnings in case the fluxes are lower then a a given threshold. The values of such thresholds are given as flux limits in Table 2.

3 Data Files Organisation and Internal Data Representation

The NASA model AE-8/AP-8 datasets are stored as arrays of integers, with common scale factors stored in the beginning of each file. This structure reduces the truncating errors and needs less storage space. The structure of the database is the same in the file and in computer memory, thus simplifying the process of loading

Table 2. Limits of NASA and INP trapped radiation models

Type of limit	AE-8/AP-8 Models Limits	INP Models Limits
Energy Range	protons - 0.1–400 MeV electrons - 0.04–7 MeV	protons - 0.1–400 MeV electrons - 0.04–7 MeV
L Range	protons - 1.15–6.6 electrons - 1.2–11	protons - 1.2–6.6 electrons - 1.2–7.0
B/B_0 Range	implicit limitation imposed by implementing atmospheric cutoff	—
B Range	—	implicit limitation imposed by implementing atmospheric cutoff
Flux Range	$\geq$10 part/cm^{2}stersec	$\geq$1 part/cm^{2}stersec

the data. The comments from source code of AE-8/AP-8 models, explaining details of data layout are given below:

```
C*************************************************************************
C************  DESCRIPTION OF MODEL DATA FILE FORMAT  ********************
C*************************************************************************
C***  THE FILE CONSISTS OF A HEADER ARRAY (IHEAD(8)) AND A MODEL MAP ***
C***  ARRAY (MAP(...)). ALL ELEMENTS ARE INTEGER.                    ***
C***                                                                 ***
C***  IHEAD(1)   MODEL MAP TYPE (SEE ABOVE)                          ***
C***       (2)   INCREMENTS PER DECADE OF LOGARITHMIC FLUX           ***
C***       (3)   EPOCH OF MODEL                                      ***
C***       (4)   SCALE FACTOR FOR ENERGY; E/MEV=E(MAP)/IHEAD(4)      ***
C***       (5)   SCALE FACTOR FOR L-VALUE                            ***
C***       (6)   SCALE FACTOR FOR B/BO                               ***
C***       (7)   SCALE FACTOR FOR LOGARITHM OF FLUXES                ***
C***       (8)   NUMBER OF ELEMENTS IN MAP                           ***
C***                                                                 ***
C***  LAYOUT OF MAP:                                                 ***
C***      MAP CONSISTS OF SEVERAL VARIABLE-LENGTH SUB-MAPS, EACH     ***
C***      FOR A DIFFERENT ENERGY. EACH SUB-MAP CONSISTS OF SEVERAL   ***
C***      VARIABLE-LENGTH SUB-SUB-MAPS EACH FOR A DIFFERENT L-VALUE. ***
C***      EACH SUB-SUB-MAP CONTAINS THE CURVE LOG(F) [DECADIC        ***
C***      LOGARITHM OF OMNIDIRECTIONAL INTEGRAL PARTICLE FLUX]       ***
C***      VERSUS B/BO [MAGNETIC FIELD STRENGTH NORMALIZED TO THE     ***
C***      EQUATORIAL VALUE]. THE CURVE IS PARAMETERIZED BY USING     ***
C***      EQUAL INCREMENTS IN LOG(F); THE NUMBER OF INCREMENTS       ***
C***      PER DECADE IS LISTED IN THE HEADER ARRAY [IHEAD(2)]:       ***
```

```
C***                                                                  ***
C***        I     B(I)/B(0)   (B(I)-B(I-1))/B(0)   LOG(F(I))        ***
C***       ------------------------------------------------          ***
C***        0       1                 -              Y              ***
C***        1     B(1)/B(0)   (B(1)-B(0))/B(0)      Y-1/IHEAD(2)    ***
C***        2     B(2)/B(0)   (B(2)-B(1))/B(0)      Y-2/IHEAD(2)    ***
C***        .       ....          .....              ....           ***
C***                                                                  ***
C***      THE SUB-SUB-MAP CONTAINS THE EQUATORIAL FLUX LOGARITHM Y    ***
C***      AND THE B/BO-INCREMENTS (THIRD COLUMN) MULTIPLIED BY        ***
C***      THEIR CORRESPONDING SCALE VALUES ( IHEAD(7) AND (8) ).      ***
C***                                                                  ***
C***  MAP(1)  NUMBER OF ELEMENTS IN SUB-MAP                           ***
C***  MAP(2)  ENERGY FOR THIS SUB-MAP; MAP(2)=E/MEV*IHEAD(4)          ***
C***    MAP(3)  NUMBER OF ELEMENTS IN SUB-SUB-MAP                     ***
C***    MAP(4)  L-VALUE FOR THIS SUB-SUB-MAP; MAP(4)=L*IHEAD(5)       ***
C***    MAP(5)  LOGARITHM OF FLUX AT EQUATOR; MAP(5)=LOG(FO)*IHEAD(7)***
C***      MAP(6)  =(B1-BO)/BO; B1 IS THE MAGNETIC FIELD STRENGTH      ***
C***              THAT CORRESPONDS TO LOG(F1)=LOG(FO)-1/IHEAD(2)      ***
C***      MAP(7)  =(B2-B1)/BO; LOG(F2)=LOG(F1)-1/IHEAD(2)             ***
C***       ...              ....                                      ***
C***      MAP(L)  LAST ELEMENT IN SUB-SUB-MAP; L=MAP(3)+2             ***
C***    MAP(I)  NUMBER OF ELEMENTS IN NEXT SUB-SUB-MAP; I=L+1         ***
C***       ...              ....                                      ***
C***     ...                ....                                      ***
C***    MAP( )  NUMBER OF ELEMENTS IN LAST SUB-SUB-MAP                ***
C***       ...              ....                                      ***
C***      MAP(K)  LAST ELEMENT IN SUB-MAP; K=MAP(1)                   ***
C***  MAP(J)  NUMBER OF ELEMENTS IN NEXT SUB-MAP; J=MAP(1)+1          ***
C***     ...                ....                                      ***
C***       ...              ....                                      ***
C***   ...                  ....                                      ***
C***  MAP( )  NUMBER OF ELEMENTS IN LAST SUB-MAP                      ***
C***     ...                ....                                      ***
C***       ...              ....                                      ***
C***      MAP(M)  LAST ELEMENT OF MAP; M=IHEAD(8)                     ***
C**********************************************************************
```

Since the computerised version of the INP models was developed only for Intel-based PC compatible computers, binary data files format was used to store database. However, for the present study, original ASCII data files were used to provide platform-independence. The database itself consists of a set of two-dimensional tables, each showing the L, B dependence of particle fluxes for a given energy. The file consists of a header of variable length, followed by the variable number of tables.

The header includes one integer number, denoting the number of energy levels for each table in the file, followed by set of floating points numbers, indicating the values of energies. Each table begins with a one-line header, containing floating point number, which gives the value of the L-shell coordinate for this table and an integer number, which gives the number of lines in this table. Each line of the table begins with a floating point number, denoting the B-value for this line of table, followed by a set of floating point flux values for this B-value, L-value, defined in the header line of the table, and energy value, defined in corresponding entry in the file header.

To simplify search procedure in tables, the routine INPINIT has been written to transform the sequence of tables into more appropriate form which is outlined in the comments to INPINIT routine, given below.

```
      FUNCTION INPINIT(FILENAME)
C      READS TABLE FROM FILE FILENAME AND FILLS
C      PENER(), PFL(), NPB(), INDP(), PMAP() ARRAYS AND NPENER,NPL VARS
C      RETURNS 0 UPON SUCCESS, <0 OTHERWISE.
C      EXPLAINATION FOR VARIABLES AND MAP ARRAYS FOLLOWS:
C
C           NPENER  - (INTEGER) NUMBER OF ENERGY VALUES IN MODEL
C                     DEFINES THE DIMENSION OF PENER() ARRAY
C           NPL     - (INTEGER) NUMBER OF L-VALUES IN MODEL
C                     DEFINES THE DIMENSIONS OF PFL(),NPB(),INDP()
C       ARRAYS
C           PENER() - ARRAY OF MODEL ENERGIES
C           PFL()   - ARRAY OF MODEL L-VALUES
C           NPB()   - (INTEGER) ARRAY, CONTAINING NUMBER OF B-VALUES
C                     FOR CORRESPONDING L-VALUE (INDICATED IN FL)
C           INDP()  - (INTEGER) ARRAY OF INDICES OF BEGINNING
C                     OF B-E MAP IN PMAP() FOR CORRESPONDING L-VALUE
C                     (INDICATED IN FL). INDP() VALUES ARE CALCUATED
C                     ITERATIVELY  USING THE FOLLOWING RULES:
C                     INDP(1)=1; INDP(I+1)=INDP(I)+NPB(I)*(NPENER+1)
C           PMAP()  - ARRAY, CONTAINING B-E MAPS.
C
C  FOR L-VALUE EQUAL TO PFL(I) IT CONTAINS:
C  PMAP(INDP(I))                        - B(1)
C  PMAP(INDP(I)+1)                      - FLUX(PENER(1),B(1))
C  PMAP(INDP(I)+2)                      - FLUX(PENER(2),B(1))
C  . . . . . . . . . . . . . . . . . . . . . . .
C  PMAP(INDP(I)+(NPENER+1))             - FLUX(PENER(NPENER),B(1))
C  PMAP(INDP(I)+(NPENER+1)+1)           - B(2)
C  PMAP(INDP(I)+(NPENER+1)+2)           - FLUX(PENER(1),B(2))
C  . . . . . . . . . . . . . . . . . . . . . . .
C  PMAP(INDP(I)+(NPENER+1)*(NPB(I)-1)) - B(NB)
```

```
C  PMAP(INDP(I)+(NPENER+1)*(NPB(I)-1)+1) - FLUX(PENER(1),B(NPB(I)))
C  . . . . . .
C  PMAP(INDP(I)+(NPENER+1)*NPB(I))     - FLUX(PENER(NPENER),B(NPB(I)))
C-----------------------------------------------------------------------
```

The datasets for the both NASA and INP models are defined as rectangular grid of points in E, L space. The grid of AE-8/AP-8 models is denser than in INP models. Note, that for protons flux models, INP grid is quite comparable to that used in the "compressed" NASA models AP-8MAC and AP-8MIC. Grid points for both sets of models are given summarised in tables 3 and 4 and plotted in Figs. 1 and 2.

Table 3. Comparison of datapoint grids for electron models

	AE-8			INP		
	Range	Step	Points	Range	Step	Points
Energy, MeV	0.04, 0.1	–	2	0.04, 0.1	–	2
	0.25 – 1	0.25	4	0.25 – 1.0	0.25	4
	1.5 – 7	0.5	12	2 – 7	1	6
	Total		18	Total		12
L	1.2–1.5	0.05	7	1.2–2.0	0.1	9
	1.6–2.0	0.1	5			
	2.2, 2.4	0.2	2	2.2, 2.4	0.2	2
	2.5 – 3.0	0.1	6	2.75	–	1
	3.2, 3.4	0.2	2	3–6	0.5	7
	3.5, 3.6	0.1	2			
	3.8–4.4	0.2	4			
	4.5, 4.6	0.1	2			
	4.8, 5.0	0.2	2			
	5.0–8.0[1]	0.5	7			
	9.0–12.0	1.0	4	8.0–11.0	1.	4
	Total		43	Total		21

Table 4. Comparison of datapoint grids for protons models

	AP-8			INP		
	Range	Step	Points	Range	Step	Points
Energy, MeV	0.1	–	1	0.1, 0.4	0.3	2
	0.2–1	0.2	5	1, 4	3	2
	2–10	2.0	5	10–50	20	3
	15	–	1			
	20–30	10	2			
	50	–	1			
	60–100	20	3	100, 200	100	2
	200–400	200	2	400	–	1
	Total		20	Total		10
L	1.12–1.14	0.02	2			
	1.15–1.17	0.02	2			
	1.2–6.6	0.1	55	1.2–3.0	0.2	10
				3.4–7.0	0.4	10
	Total		59	Total		20

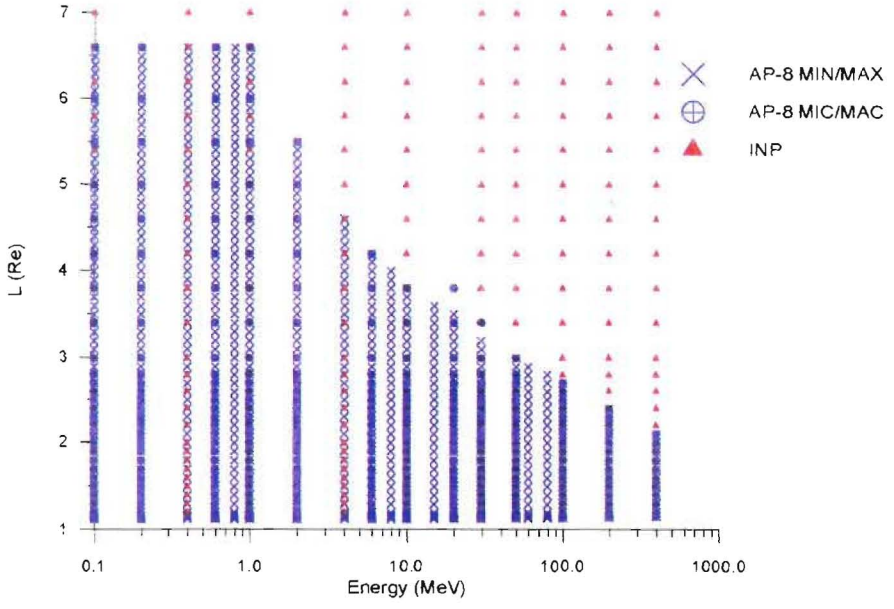

Figure 1. E, L grid of NASA and INP proton models

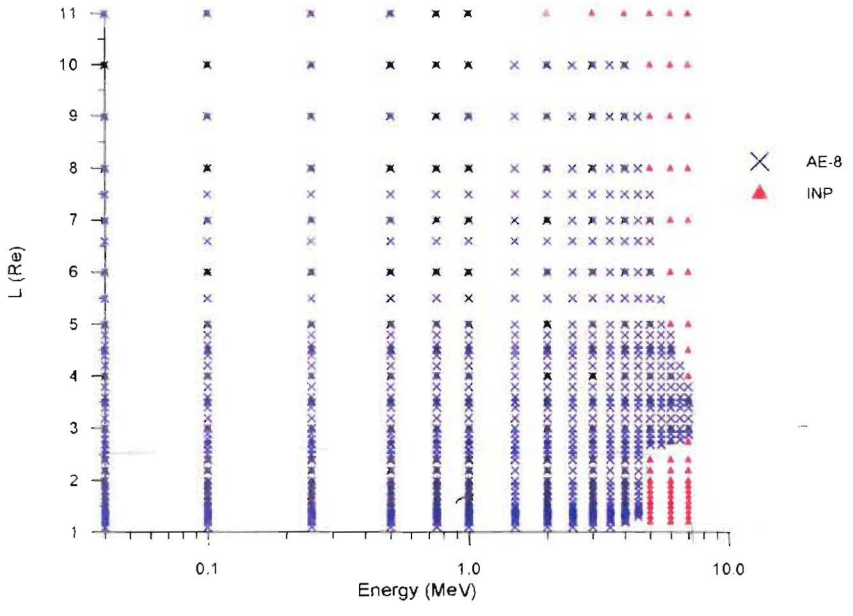

Figure 2. E, L grid of NASA and INP electron models

4 Interpolation Methods

To interpolate between grid points in AP-8/AE-8 models, the FORTRAN programs, `TRARA1` and `TRARA2`, are generaly used. `TRARA1` performs linear interpolation of fluxes logarithms in the energy space, while `TRARA2` performs linear interpolation of fluxes logarithms in $L, B/B_0$ space. `TRARA2` was briefly described by Teague et al. (1972) and method of interpolation used in `TRARA2` was expained in details by Vette (1991a). The general idea behind the method used in `TRARA2`, is to find two radial straight lines in $B/B_0, \log(\text{flux})$ space which pass through models datapoints and are as close as possible to the point, whose coordinates are given values of L and B/B_0. A better method of interpolation was introduced recently by Daly & Evans (1993) which is implemented in their `TRARAP` subroutine.

Interpolation method used in the INP models is less sophisticated and more straightforward if compared with those used for AE-8/AP-8 models. Linear interpolation is performed for B and L, while logarithmic interpolation is performed for E. The type of the interpolation, and the number of interpolations made for each flux calculation in INP models are given in the Table 5.

Table 5. Use of interpolation in INP model

Coordinate	Type of interpolation	Number of interplations, for one flux calculation
B	linear	4
E	logarithmic	2
L	linear	1

The interpolation subroutine used in the INP models is called `FINTL1`. First linear interpolation in B is made for two pairs of points for different E. Then logarithmic interpolation is performed in E using values obtained in the previous step. Then the same interpolation is performed for a different L, and finally linear interpolation in L-space is made, using results from the previous steps. This method seemed to be the simplest way to obtain data from the model. However, because of the triple interpolation it may be the source for the interpolation errors.

Chapter 3

Comparison of Fluxes

1 Introduction

To compare the fluxes of each model, the quantities $\log(J_{\mathrm{INP}}/J_{\mathrm{NASA}})$ were calculated for each pair of corresponding models: INP-ELECMIN with AE-8MIN, INP-ELECMAX with AE-8MAX, INP-PROTMIN with AP-8MIN, INP-PROTMAX with AP-8MAX. The ranges of energy, L and B wherein both models are compared, are given in Table 6.

Table 6. Region of comparison of INP and NASA models

	Electrons	Protons
Energy Range Logarithmic grid	0.04–10 MeV	0.1–1000 MeV
L Range Linear grid	1.2–11	1.2–6.6
B/B_0 Range Linear grid	1–60	1–60

While calculating the ratio $\log(J_{\mathrm{INP}}/J_{\mathrm{NASA}})$, the lower limits of model fluxes were taken into account ($J_{\mathrm{INP}} \geq 1$ part/cm^2 sec, $J_{\mathrm{AE-8/AP-8}} \geq 10$ part/cm^2 sec). The values of this ratio are stored in a binary file, which will be later accessed by a PV-WAVE program to plot color map of the log of ratio as function of any pair of coordinates, the third coordinate being fixed. These maps were built using `TRARAP` subroutine to interpolate between grid points in NASA models. Note that full datasets full datasets of AP-8 models (AP-8MAX and AP-8MIN) were used instead of "compressed" versions AP-8MAC and AP-8MIC. To perform interpolation in B/B_0, using the INP models, the FORTRAN subroutine `FINTL1B0` was written. It

first calculate B/B_0 value, using equatorial B values stored in the model, and then calculate B value from given B/B_0.

An example of such a plot for protons equatorial fluxes ($B/B_0 = 1$) and for solar maximum is shown in Fig. 3. The solid contour lines of flux map for the AP-8MAX model are also shown on the map. For all other two-dimensional map similar contour lines are plotted; they correspond to the flux value of the second model, named in the title. Value of the ratio of log fluxes is chosen to accomodate for the large dynamic range of the models in the region of comparison. Shading in red color on the map indicates the points where flux given by INP model is higher than in the corresponding NASA model; blue color indicates that the NASA model returns a higher flux. Points of the map, for which one or both models return flux below their respective thresholds were shaded with gray color. It should be noted that for each map the color palette was scaled differently, so that the color range covers the whole range of ratio values from minimum to maximum values. Therefore, when comparing different figures, attention should be paid to the values shown in the color legend of the map.

Vette (1991b) estimate that the errors in NASA models are "about a factor of two". He also noted that "the greatest error should be expected where steep gradients in spatial or spectral distributions exist". Therefore, we will also consider here, that when the fluxes of INP and NASA models agree within the factor of two or less (i.e. absolute value of logarithm of flux ratio less then 0.3) the models are in satisfactory agreement with each other.

The comparison between the full and "compressed" in the NASA models can also be made with the software which has been developed during this study. Comparison of results obtained with `TRARA2` and `TRARAP` for the same model is also possible with the same software.

2 Equatorial fluxes

Results of comparison for equatorial fluxes ($B/B_0 = 1$) are shown on Figs. 3–6.

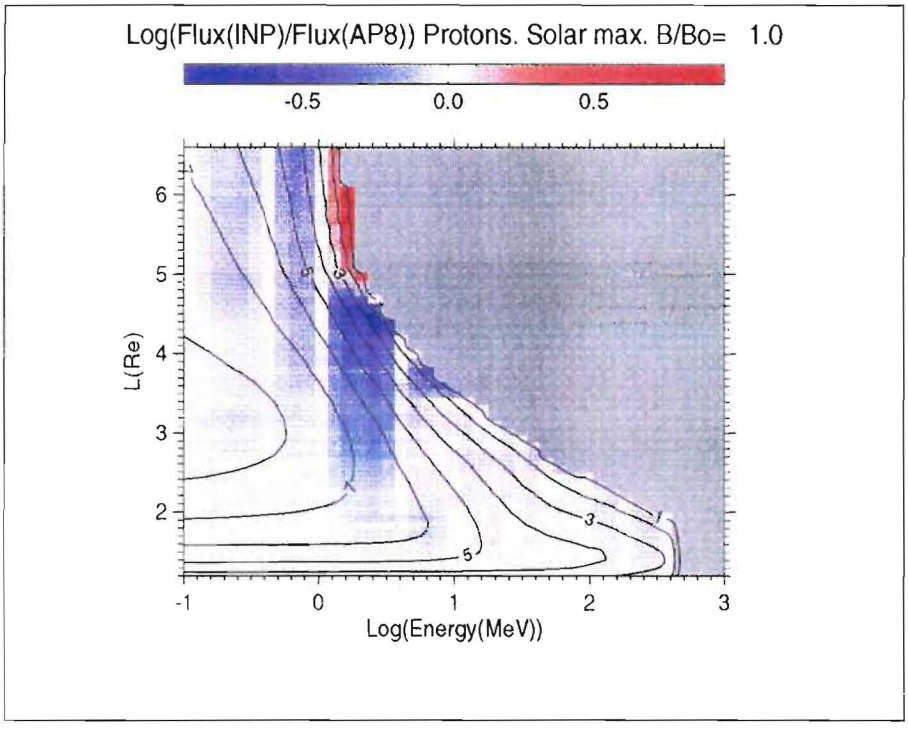

Figure 3. Comparison of proton equatorial fluxes during solar maximum

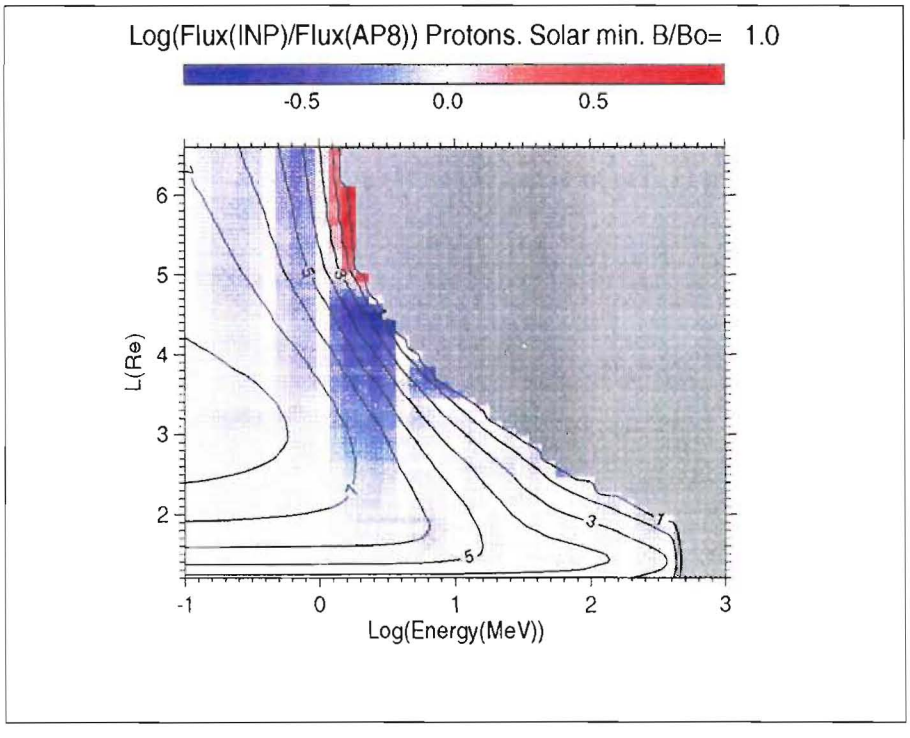

Figure 4. Comparison of proton equatorial fluxes during solar minimum

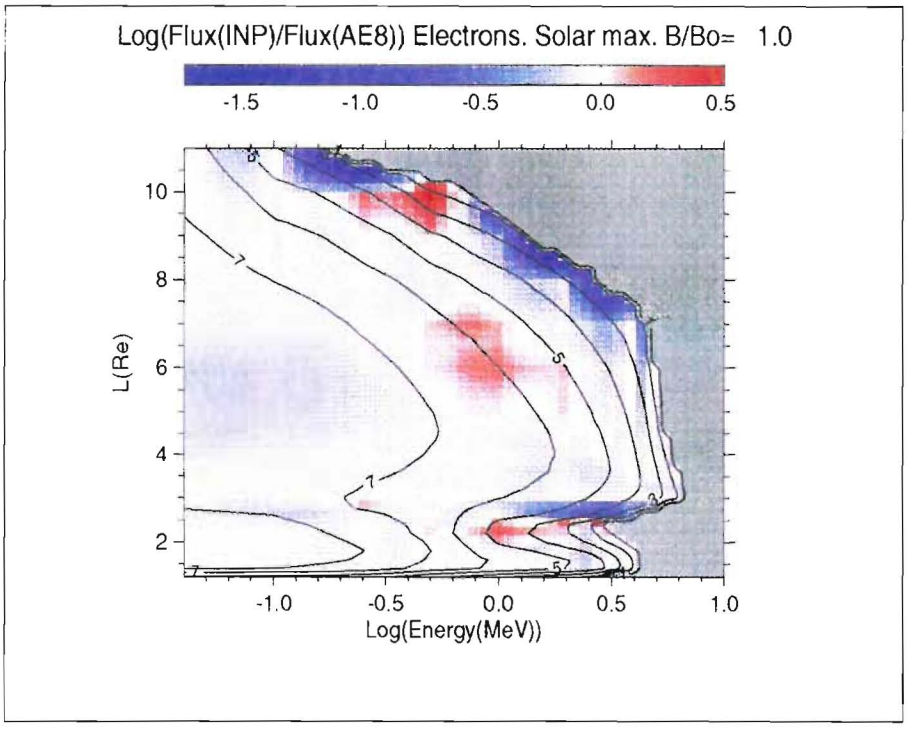

Figure 5. Comparison of electron equatorial fluxes during solar maximum

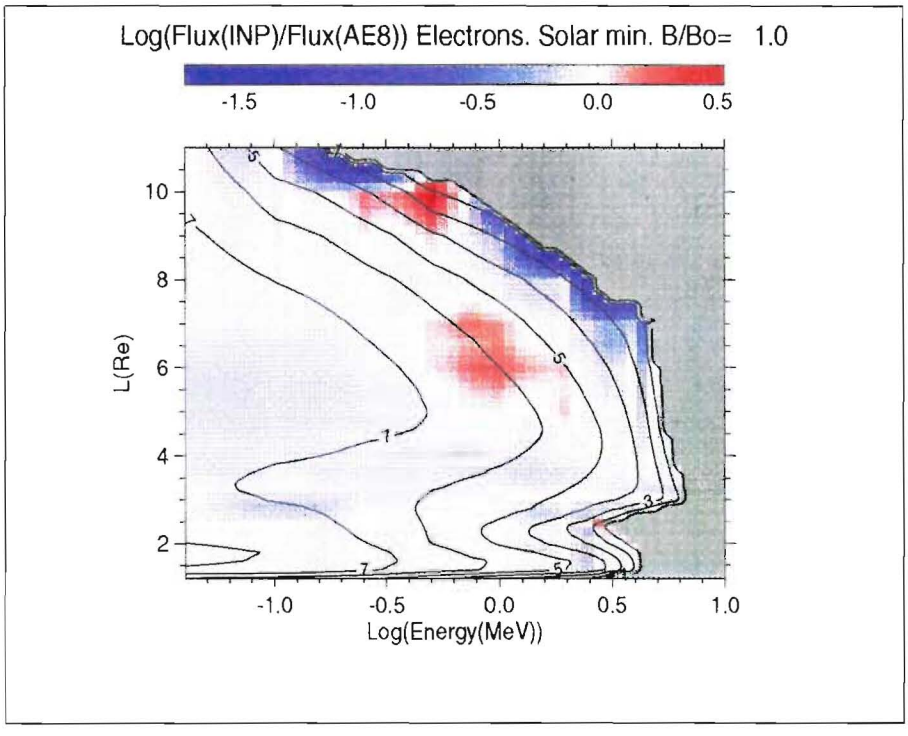

Figure 6. Comparison of electron equatorial fluxes during solar minimum

Figs. 3 and 4 compare INP and NASA proton models for solar maximum and solar minimum respectively. These figures illustrate the relatively good agreement between INP and AP-8 models. For most E, L space the difference is less then a factor of two which means that $\log(J_{\mathrm{INP}}/J_{\mathrm{AP-8}}) < 0.3)$. However, a one order of magnitude difference is observed in the region of steep gradients close to the outer border of radiation belt. Brighter vertical strips, observed at energy values 0.4, 1, 4 and 10 MeV correspond to the values of energies common in the NASA and in the INP models (see Table 4 and Fig. 2). This indicates that larger discrepancies between models are formed in the regions where the grid is sparser in the INP model because of the different interpolation methods used.

In most parts of E, L space the difference between logarithms of electron fluxes (Figs. 5 and 6) does not exceed 0.1. There are larger differences, however, in the region of the gradients. In most cases INP model underestimate the fluxes, compared with AE-8 model except for a small region around $E = 500$ keV and $L = 10$, where INP model fluxes are half an order larger that those of AE-8MIN and AE-8MAX. These discrepancies occur in proximity of the boundary of applicability of AE-8 where the accuracy of AE-8 itself is about an order of magnitude. It can therefore concluded that both models give results which is consistent with each other in the region where the flux is large enough and where the gradients are not too steep.

The comparison can also be made taking into account the statistical standard deviation $\sigma_{\mathrm{AE-8}} = \sigma[\log(J_{\mathrm{AE-8}})]$, defined in AE-8 model for $L > 3$. The color maps in this case were produced for the value $\log(J_{\mathrm{INP}}/J_{\mathrm{AE-8}})/\sigma_{\mathrm{AE-8}}$. Gray shading covers the region of space where one or both models are undefined or where $\sigma_{\mathrm{AE-8}}$ is undefined. These color maps for equatorial fluxes are shown in Figs. 7 and 8 respectively for solar maximum and minimum. Both models produce results to be within $\pm\sigma_{\mathrm{AE-8}}$ everywhere, except for $L > 6$ where $\sigma_{\mathrm{AE-8}}$ becomes too small. Differences shown in the region of steep gradients could be explained by differences in interpolation methods.

It can be concluded that near the geomagnetic equator both models produce comparable results. The largest discrepancies are found in the region of steep gradients where different methods of interpolation and different networks of grid points lead to different interpolated fluxes. The limited amount of observations in this region of the magnetosphere as well as small values of the observed flux and thir variability in time is probably the reason for these large local discrepancies. One can also incriminate the $B/B_0, L$ coordinate system which becomes more inadequate at $L > 6$ when no external magnetic field is used to determine B and L.

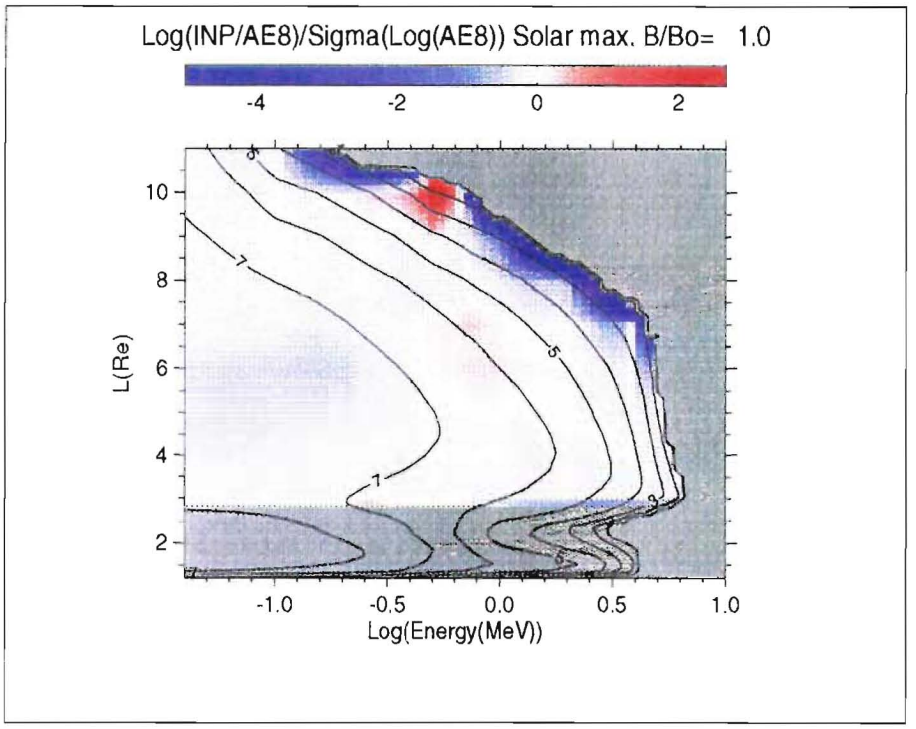

Figure 7. Comparison of electrons equatorial fluxes relative to AE-8 standard deviation during solar maximum

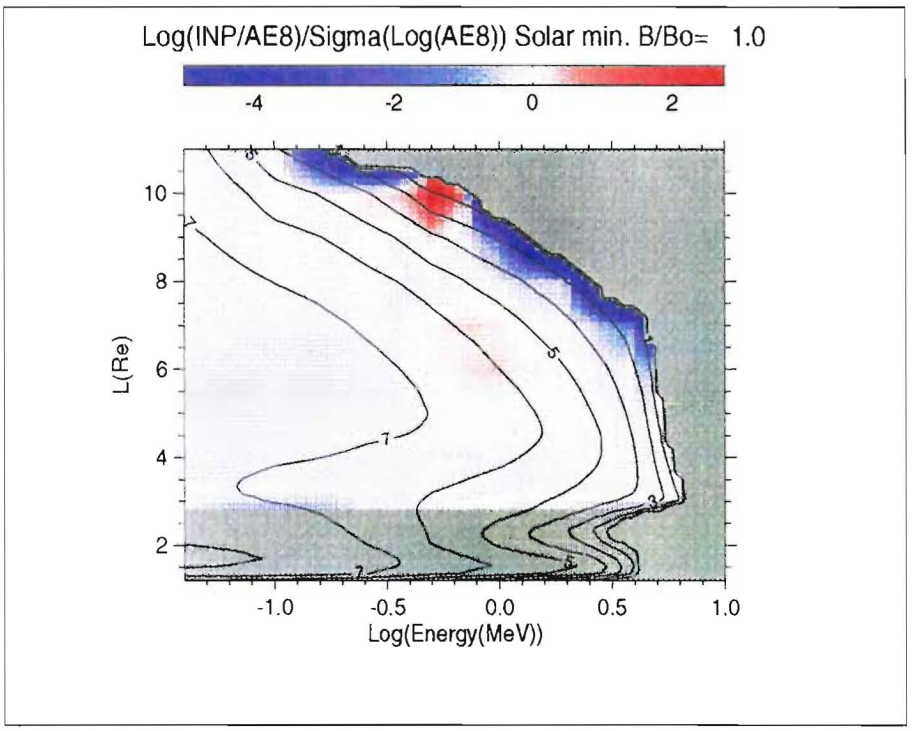

Figure 8. Comparison of electrons equatorial fluxes relative to AE-8 standard deviation during solar minimum

3 Off-equator fluxes

To compare the models away from the geomagnetic equator the color maps were produced for the constant energy values, $E = 2$ and 100 MeV for protons; $E = 0.5$ and 2 MeV for electrons. These plots for solar minimum are shown on Figs. 9–12). The low-L border where the flux of particles decreases rapidly to zero corresponds to the atmospheric cutoff. When L increases B_c/B_0 increases as $0.66L^{3.452}$, which corresponds to Vette's cut-off definition (Daly & Evans 1993). In the NASA models B_c corresponds to the magnetic field at an altitude of 100 km. Since INP models were prepared using the data based on NASA models, both models have similar cutoff values.

From the comparison of protons fluxes (Figs. 9 and 10) it can be concluded that the difference between models are much larger at lower energies than at higher energies. For example for 2MeV protons fluxes the INP models underestimate fluxes compared with the NASA models in most part of the radiation belts. For 100MeV protons the comparison gives agreement well below of factor of two difference, except in the region of atmospheric cutoff.

The comparison of electrons fluxes (Figs. 11–13) shows that much better agreement is found in the region of inner electrons belt ($L < 2.5$ in Fig. 12) than in the region of outer electron belts. Again a poor agreement is observed at the edges of the radiation belts, where the gradients of flux are largest. Note that both models differ significantly between $L = 2.5$ and 3. The largest discrepancies are found for solar maximum conditions. For solar maximum the INP models electrons flux in this region is an order of magnitude lower, compared with AE-8MAX model.

It should be noted, that the "pattern" of differences between models are different on the geomagnetic equator ($B/B_0 = 1$, left edge of the maps on Figs. 9, 12) and the region $B/B_0 > 1$. This difference can be explained by the fact that for equatorial flux calculations, interpolation in B/B_0 space is not necessary, since both models contains equatorial flux values. As the one moves to higher B/B_0 values, additional interpolations should be made, which bring in additional discrepancies.

Color maps of fluxes ratio versus E and B/B_0 have also been produced for a constant $L = 6.6$. These maps for protons and electrons fluxes are shown on Figs. 14, 15 for solar minimum . In Fig. 14 bright vertical stripes are seen at the energy values, corresponding to those where the energy grid points of the INP models coincides those of NASA ones (see Fig. 2). For other energies where interpolated values are compared larger differences are observed. This shows again the importance of interpolation methods used in retieving fluxes from tabulated empirical models.

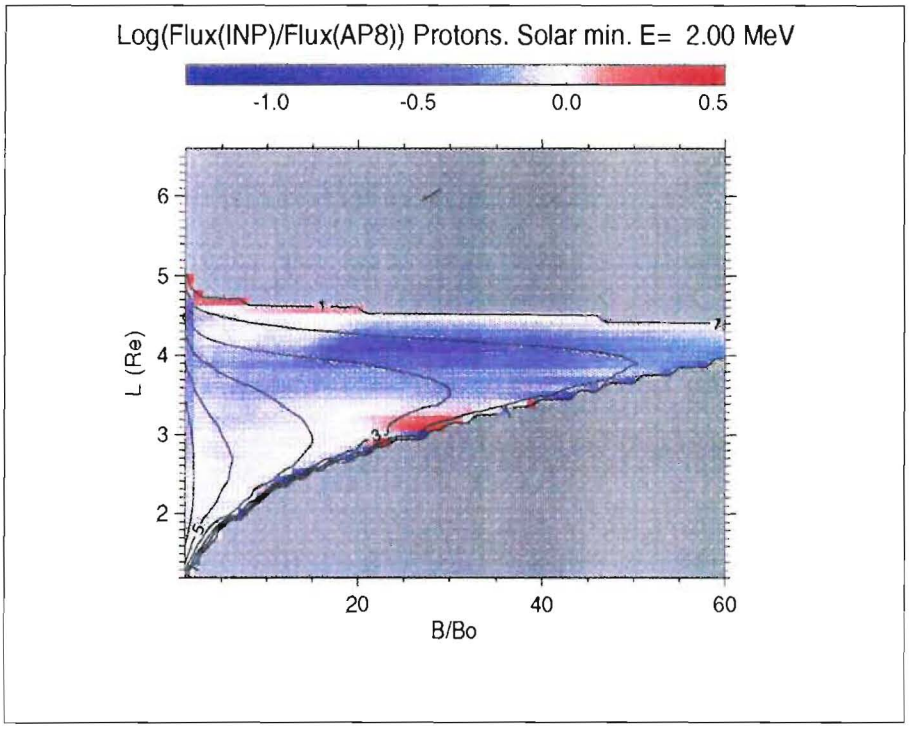

Figure 9. Comparison of 2 MeV proton fluxes during solar minimum

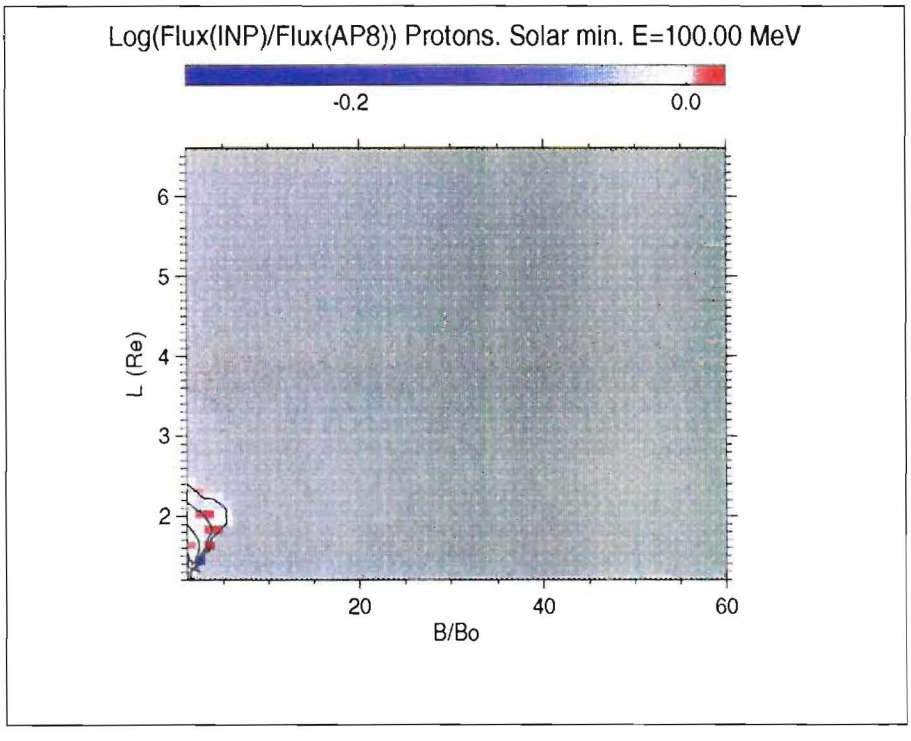

Figure 10. Comparison of 100 MeV proton fluxes during solar minimum

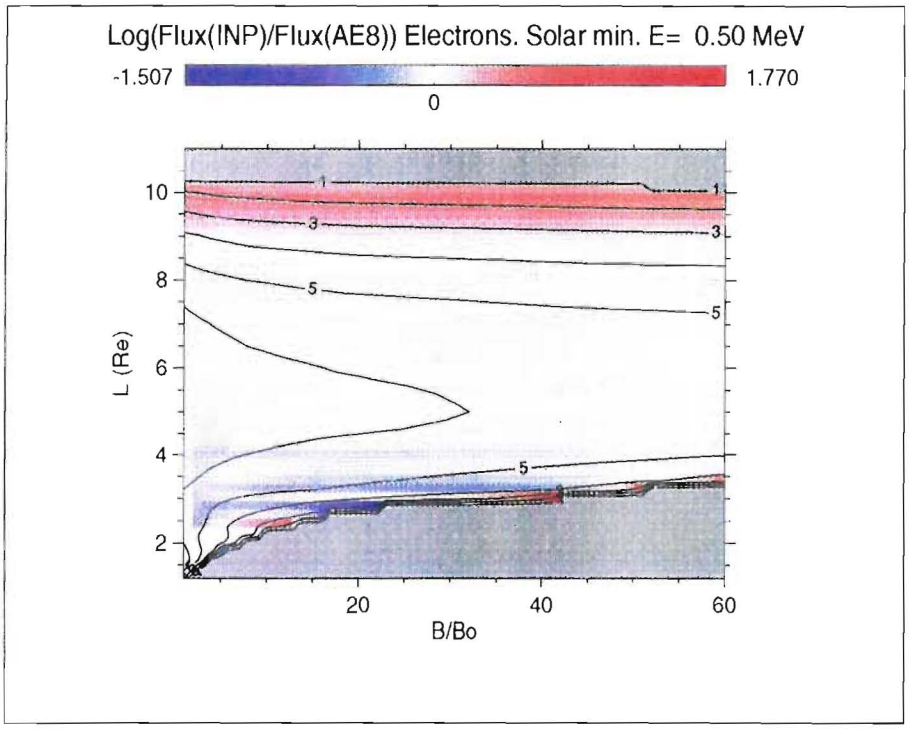

Figure 11. Comparison of 0.5 MeV electrons fluxes during solar minimum

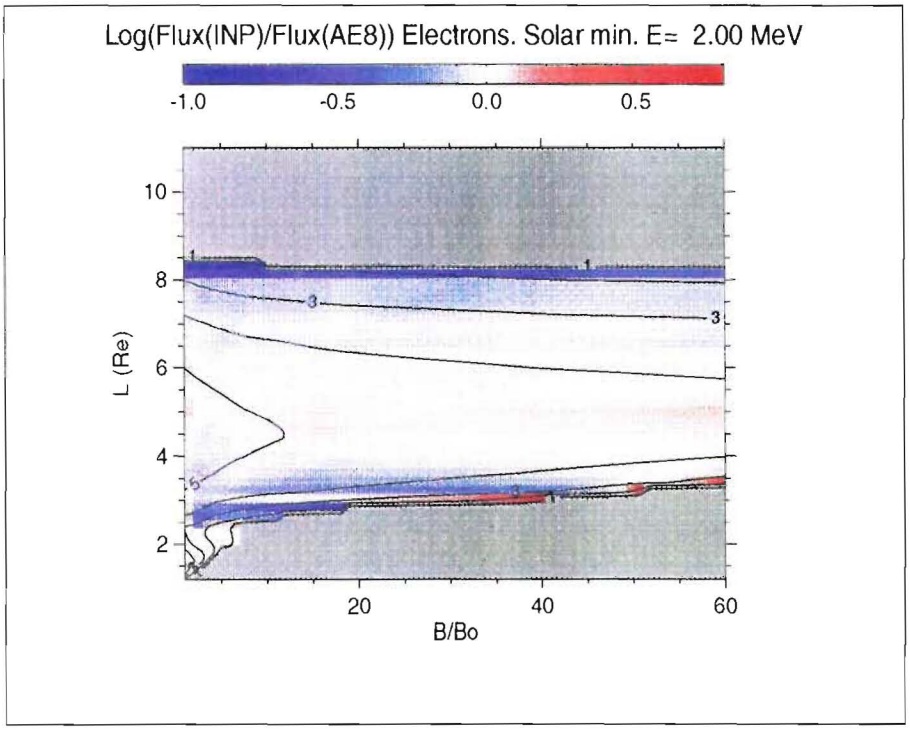

Figure 12. Comparison of 2 MeV electrons fluxes during solar minimum

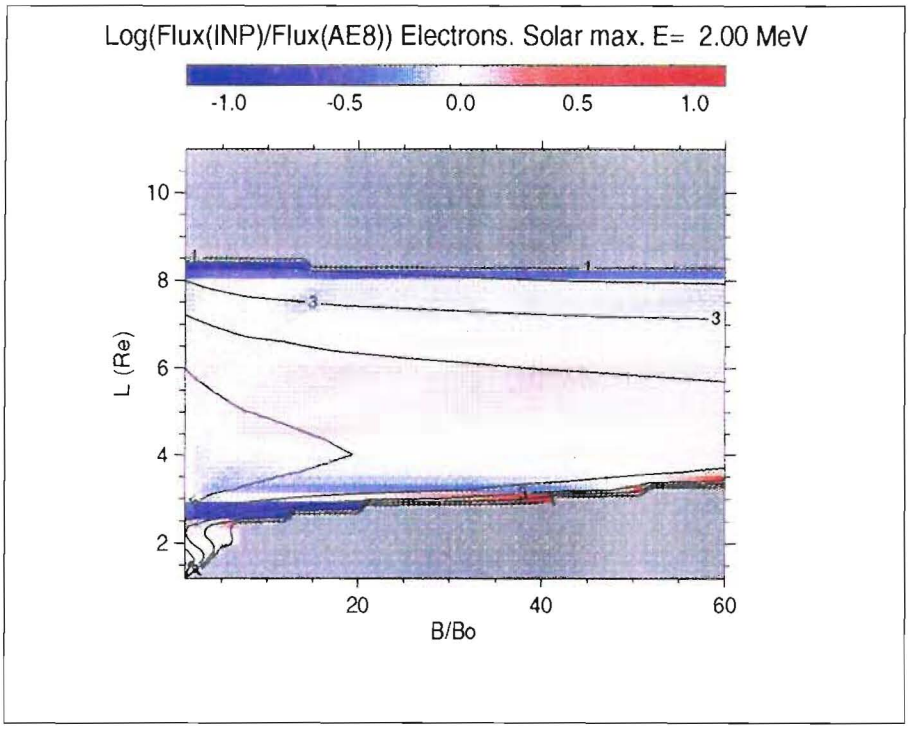

Figure 13. Comparison of 2 MeV electrons fluxes during solar maximum

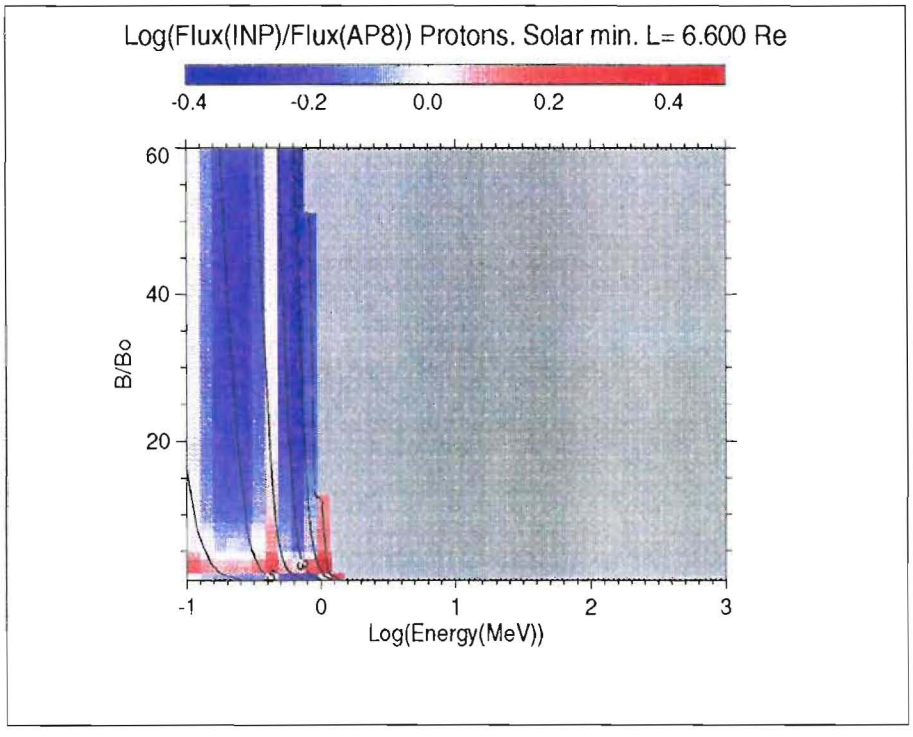

Figure 14. Comparison of proton fluxes for $L = 6.6$ during solar minimum

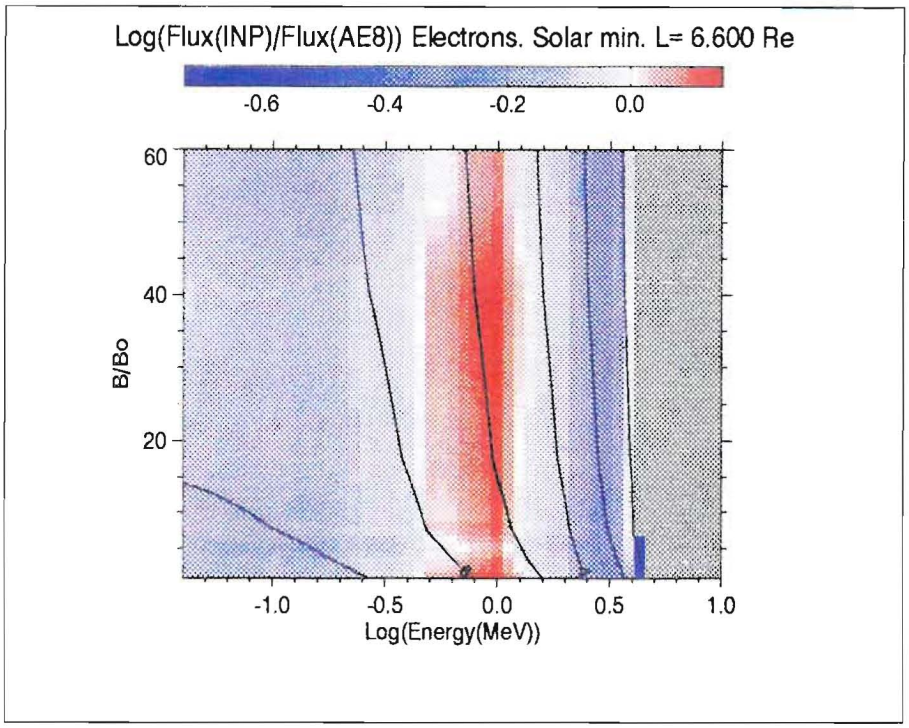

Figure 15. Comparison of electron fluxes for L=6.6 during solar minimum

Fig. 15 shows that small corrections (less then a factor of two) were introduced in the INP electrons models at $L = 6.6$ and energies 0.5–1 MeV. The discrepancies in this region cannot be explained by interpolation, since both models have similar grid spacing in this region (see Fig. 2). However these changes are small and differences are most of the time well inside the range of uncertainty of the NASA model.

It can be concluded from the comparison, that some differences between the NASA and INP electrons models exist in limited regions of E, L, and B/B_0, (e.g. for E =500 keV–1 MeV and L = 6.6, and, for L =2.5–3.0 for solar maximum). Otherwize these models show reasonable agreements with each other.

4 Solar cycle variations

To compare the behaviour of both models during solar cycle the same color maps were produced for the value $\log(J_{\mathrm{MAX}}/J_{\mathrm{MIN}})$. Here J_{MAX} and J_{MIN} denote values of flux calculated, using the model for the maximum and minimum of solar activity, respectively. This is done for both the NASA and INP models. Such plots were produced for pairs of models AP-8MAX vs. AP-8MIN, AE-8MAX vs. AE-8MIN, INP-PROTMAX vs. INP-PROTMIN, INP-ELECMAX vs. INP-ELECMIN for equatorial fluxes (Figs. 16–19).

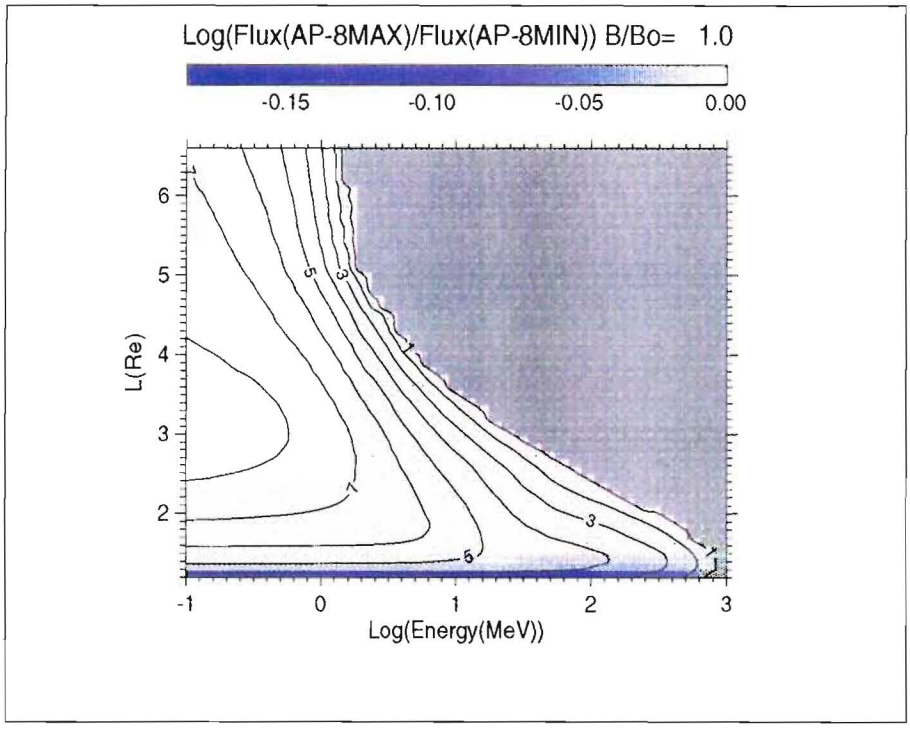

Figure 16. Solar cycle variations of AP-8 model equatorial flux

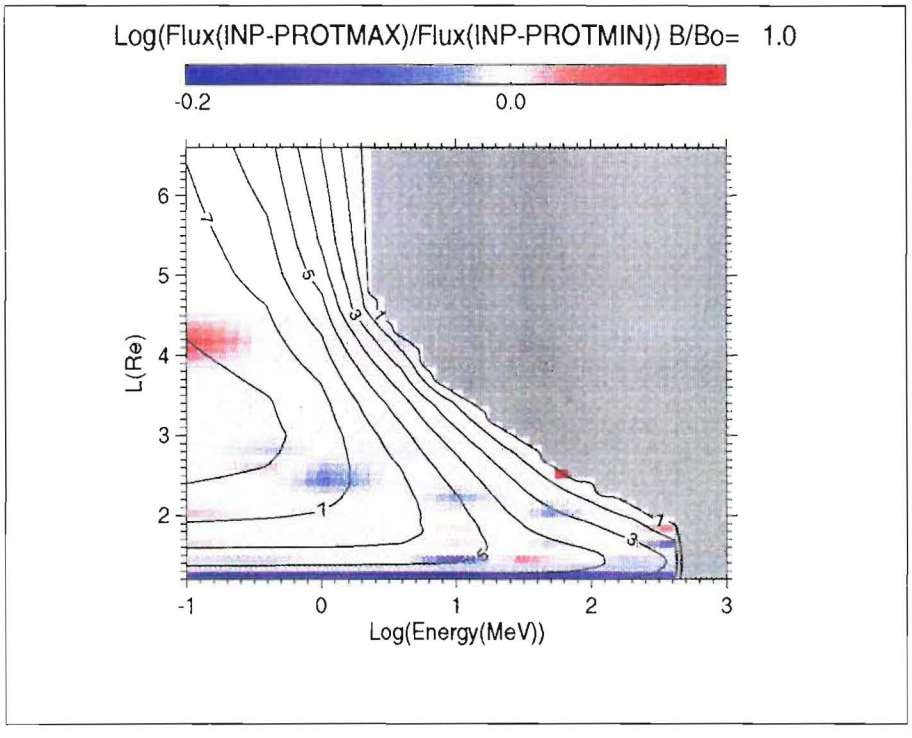

Figure 17. Solar cycle variations of INP model proton equatorial flux

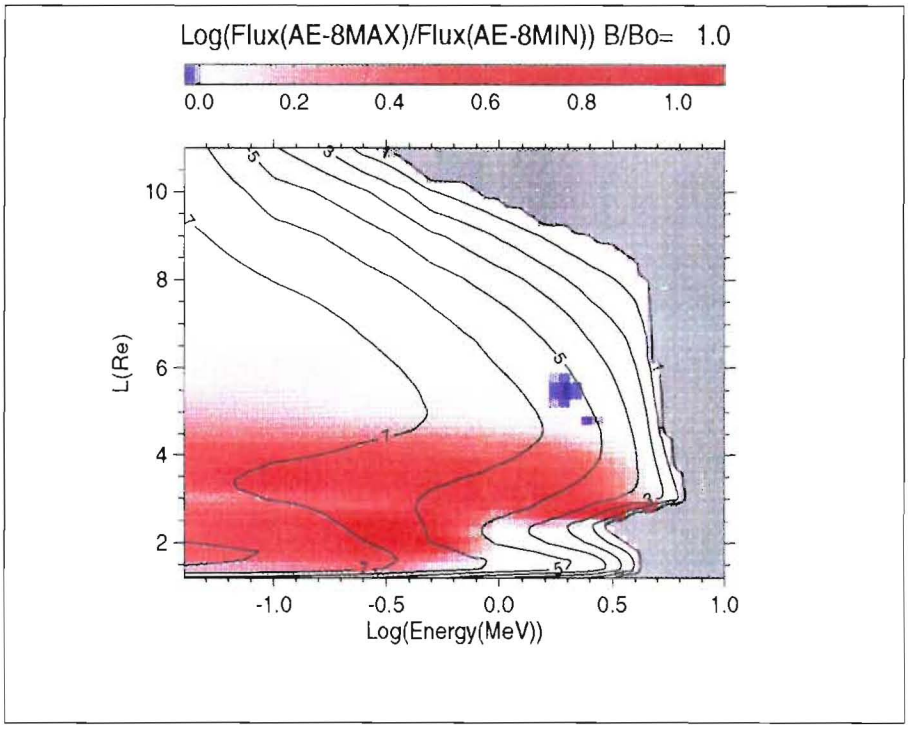

Figure 18. Solar cycle variations of AE-8 model equatorial flux

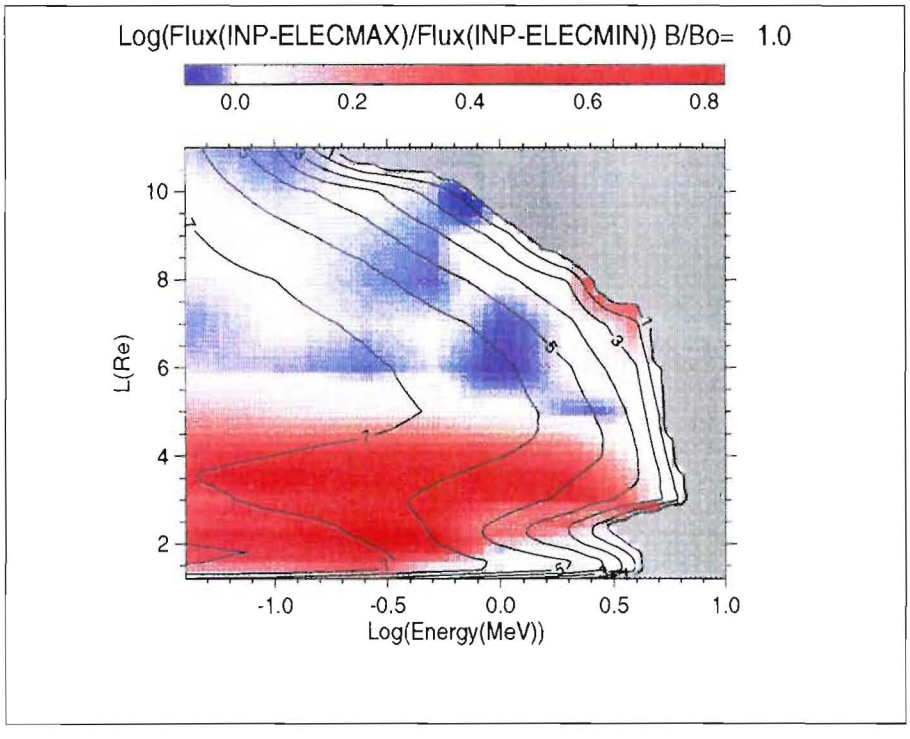

Figure 19. Solar cycle variations of INP model electron equatorial flux

It can be seen from Fig. 16 that AP-8 models for protons have the same equatorial fluxes during solar cycle, except in a very narrow region near the atmospheric cutoff, where the fluxes are smaller for the AP-8MAX model. The values of flux difference between solar maximum and minimum corresponds to those, described by Sawyer and Vette (1976).

INP protons flux models also show the same feature. Additional small variations of flux during solar cycle across the whole trapped radiation belt region can be seen in Fig. 17. This can be explained by the fact, that the fluxes at data points in the INP models are given with the accuracy of only three digits. Round-off errors together with interpolation can produce the small variations of the flux found on Fig. 17.

Comparison for the electrons models (Figs. 18, 19) shows, that in the region of $L < 5$ both the NASA and INP models produce similar flux variations over the solar cycle. For most energies in this region the flux during solar maximum is about a factor of 6 larger than during solar minimum. The flux in the region of $L > 5$ remains constant in AE-8, while showing small variations in the INP models, similar to those in the INP protons models.

Figs. 20 and 21 were produced for the constant protons energy $E = 10$ MeV. They illustrate that both the INP and the NASA models have the solar cycle flux variations at all points along magnetic field lines. Fig. 22 shows the ratio of INP-PROTMAX/INP-PROTMIN fluxes for the constant energy of 1 Mev. The red "spot", seen around $L = 5.5$ and $B/B_0 = 5 - 10$ is due to the fact that additional satellites data have been used in this region to update one of INP models. However this difference is rather small(a factor of 2 at most).

Figs. 23 and 24 are obtained for a constant electron energy of 2 MeV. It can be concluded that electrons fluxes in both models have similar field aligned dependences. Again one can clearly see the small discrepancies, which we attribute to round-off errors (blue spots in Fig. 24 and a blue stripe in Fig. 23.) The difference of red color intensity in the area $L = 2.5$–3 with nearly identical color scale on both maps can serve as confirmation that electron fluxes of the INP model differs from those in the AE-8 model for this region. (see Figs. 12 and 13).

The color map, displayed in Fig. 25 shows the ratio of fluxes in INP electrons models at solar maximum and minimum for constant $L = 6.6$. We explain the observed pattern as the result of the interpolation. This can serve as a good illustration of the disadvantages of the method of interpolation selected for the INP models.

It can be concluded from the comparison of solar cycle variations, that both NASA and INP models show similar dependencies for the fluxes. Comparison between models for solar minimum and solar maximum points out the differences between models, despite the interpolation errors, since in this case the impact of interpolations errors is minimised.

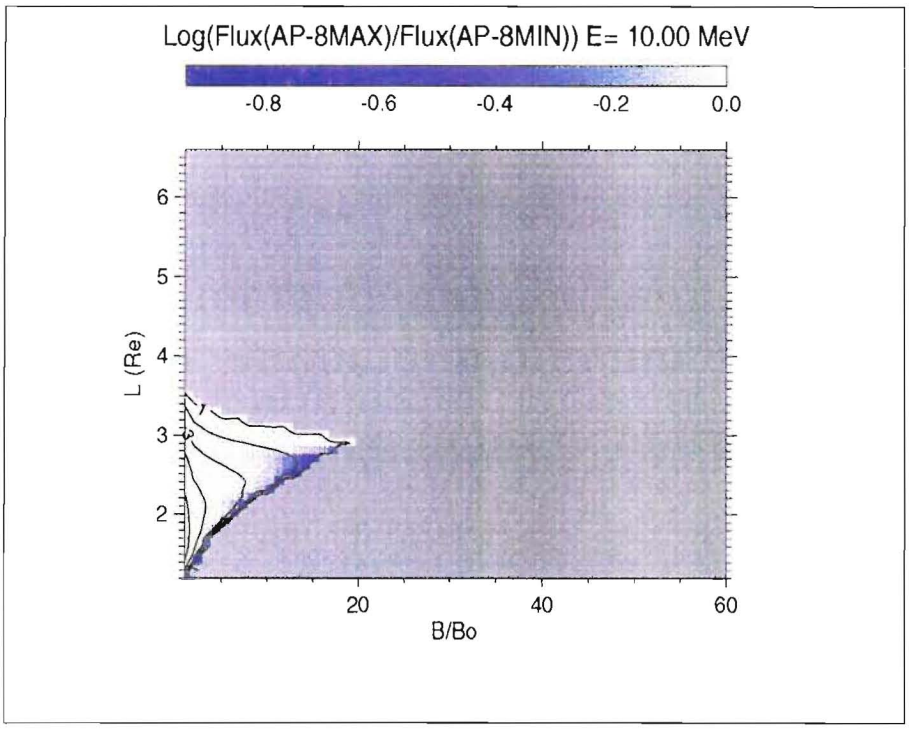

Figure 20. Solar cycle variations of AP-8 model for 10 MeV proton flux

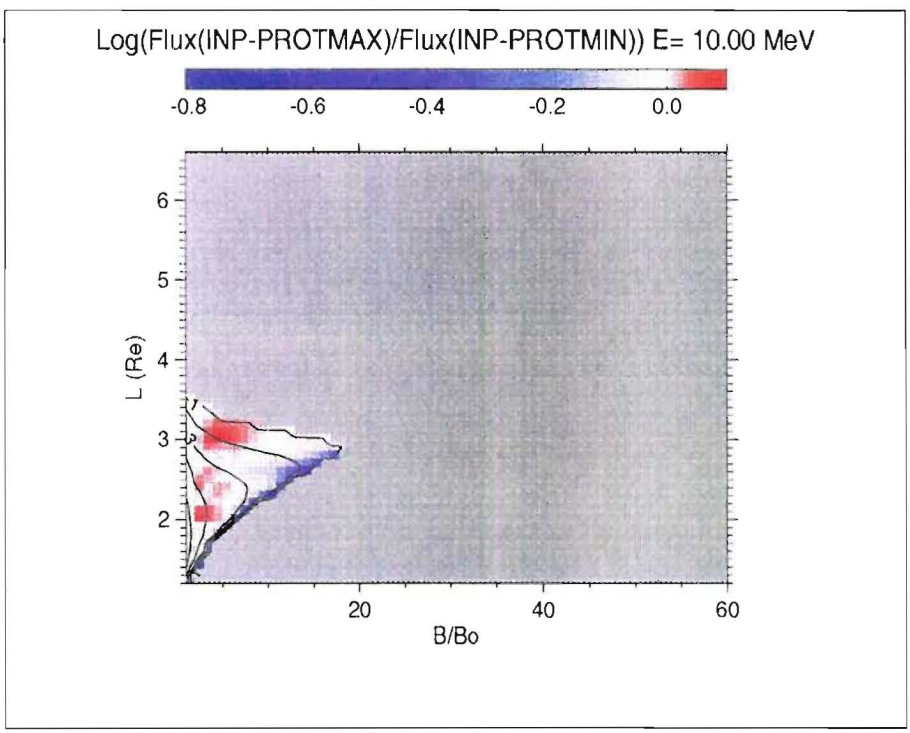

Figure 21. Solar cycle variations of INP model for 10 MeV proton flux

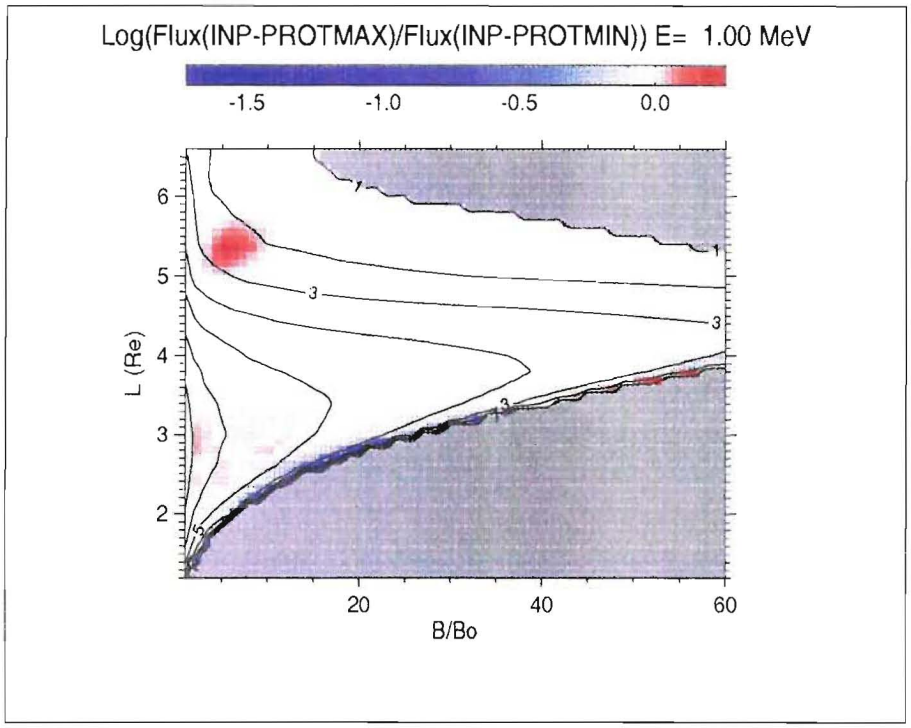

Figure 22. Solar cycle variations of INP model for 1 MeV proton flux

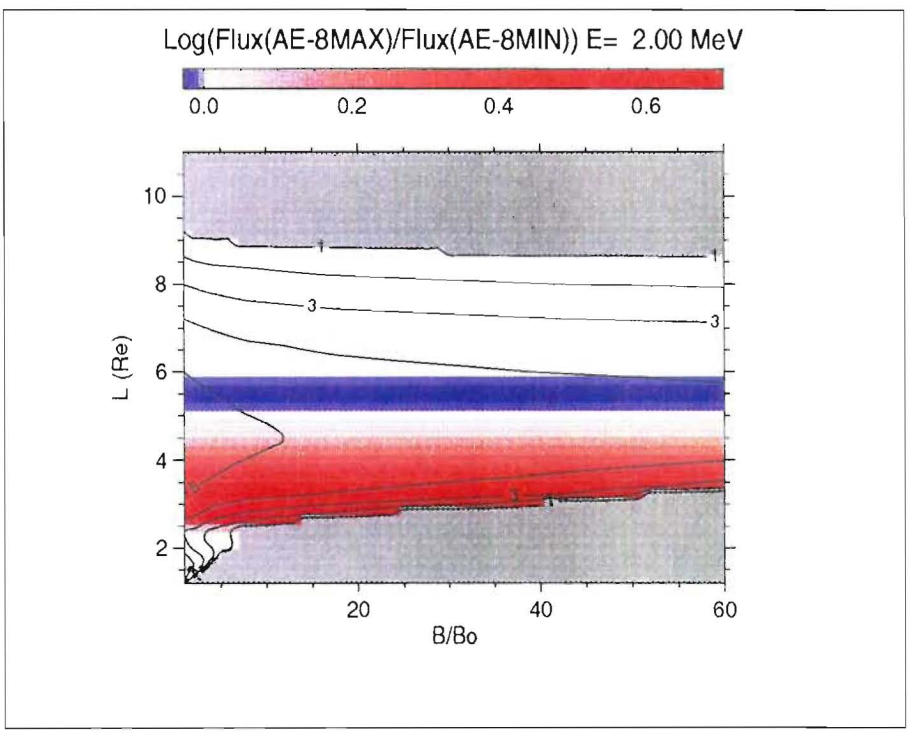

Figure 23. Solar cycle variations of AP-8 model for 2 MeV electron flux

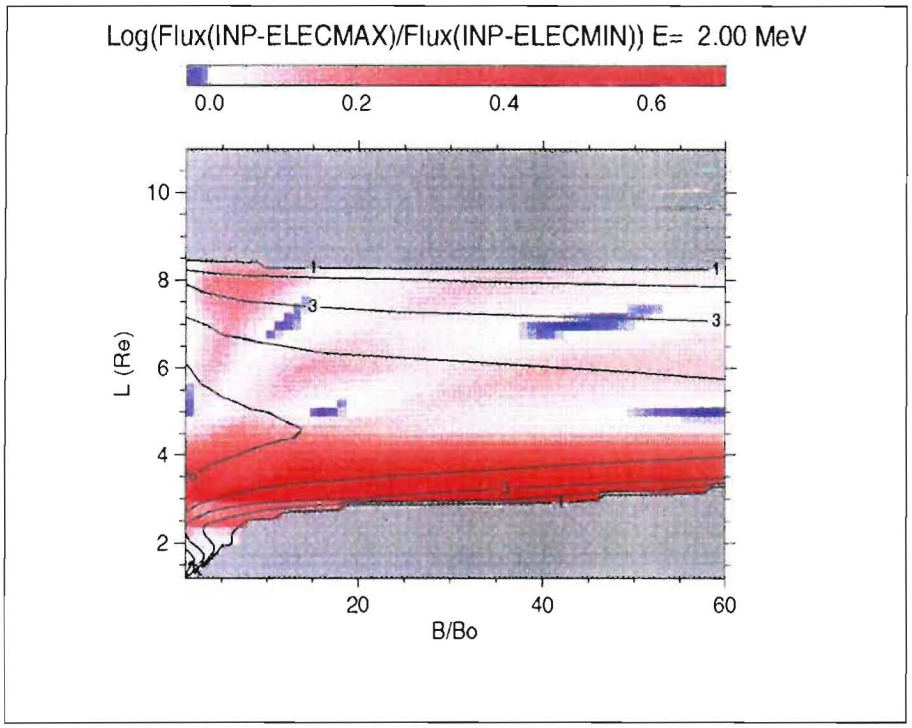

Figure 24. Solar cycle variations of INP model for 2 MeV electron flux

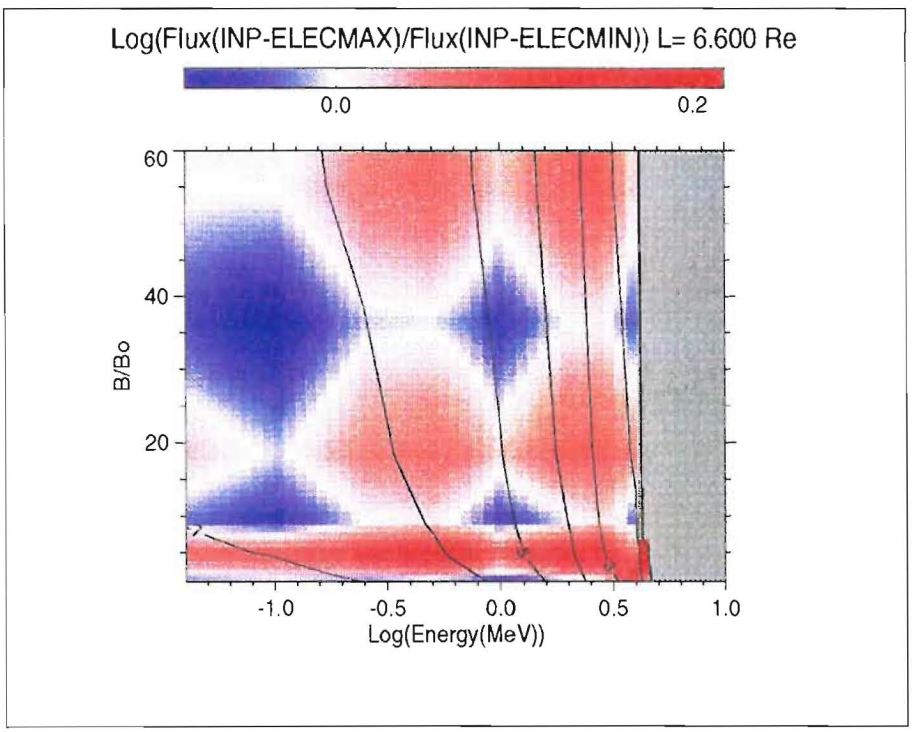

Figure 25. Solar cycle variations of INP model for electron flux at L=6.6

5 Fluence Comparisons

To study the differences in NASA and INP models the calculations of daily particle fluence for LEO orbit were performed using both models. The fluence calculations were made for the circular orbit with the altitude of 500 km and inclination 51.6° (one of possible orbits for a Shuttle-Mir mission). Positions of spacecraft in geographical and B, L coordinates were calculated for each 30 seconds during 24 hours, using UNIRAD software. The Jensen and Cain (1960) magnetic field model and GSFC12/66 model, updated to 1970, were used to calculate L and B coordinates for electrons and protons respectively, as recommended by Heynderickx et al. (1994). Daily fluences for the set of energy values were then calculated for those B, L coordinates using both NASA and INP models for solar maximum. The resulting fluences for protons and electrons are shown on Figs. 26 and 27 respectively. The results show good agreement between daily fluxes calculated by INP and NASA models. It should be noted, that most of this orbit is located close to the atmospheric cutoff in the region of steep flux gradients and, correspondingly large discrepancies between models. However, the averaging along the orbit produce the fluences with the difference at most a factor of two.

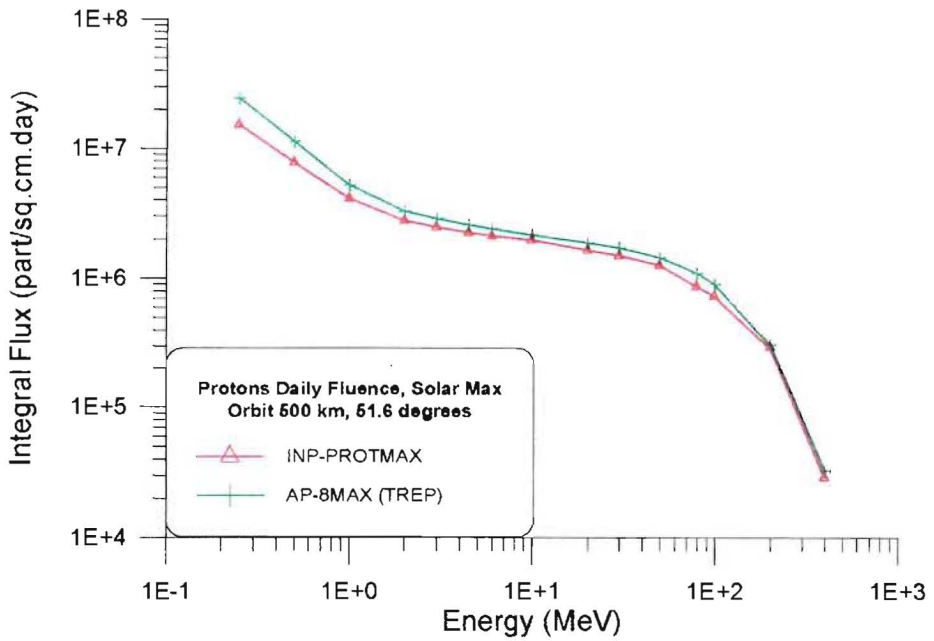

Figure 26. Daily proton fluence according to the NASA and INP models

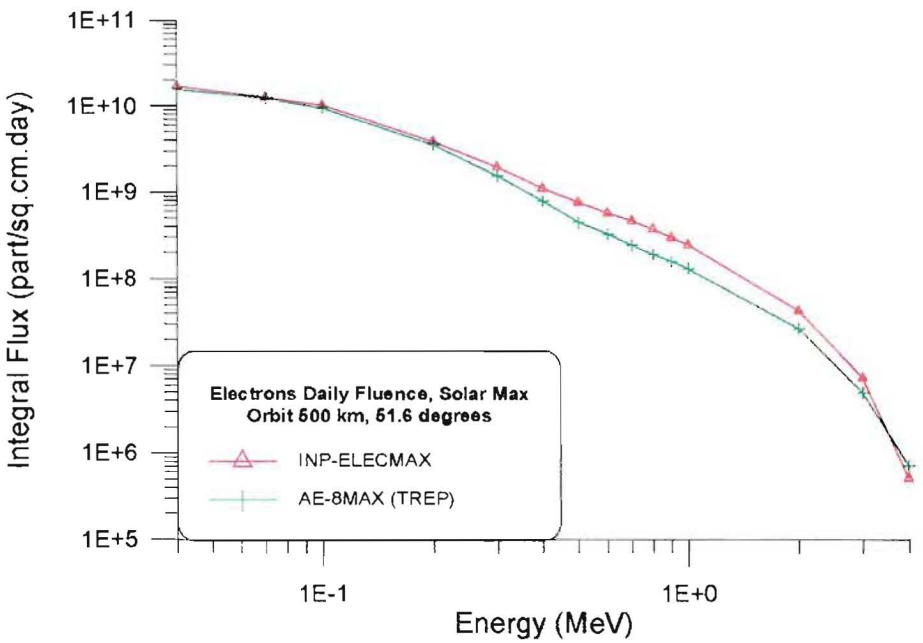

Figure 27. Daily electron fluence according to the NASA and INP models

Conclusions

The trapped radiation models developed at the Institute of Nuclear Physics (MSU) and at NASA, use different interpolation methods and different grids of points to store the data. However, it can be concluded from the comparisons made in the present study, that both NASA and INP trapped radiation models produce similar fluxes in the bulk of the Earth's radiation belts region where the largest fluxes are observed and where the gradients are not too large. There are differences between models in limited range of L, E, and B/B_0, such as for electrons fluxes during maximum for $L = 2.5$–3.

In the region of steep gradients, there are significant differences between models. One of the reasons for such discrepancy is the different choice of B or B/B_0 coordinate to organise respectively the INP and the NASA models. Indeed, at low altitudes B/B_0 varies less, then B as a function of altitude. Future trapped radiation models should be organised in another coordinate such as ϕ (Daly & Evans, 1993) or the Hassitt (1965) shell height.

The present study also showed that there is a need for "standardizing" the models, i.e. specifying the methods of storing and accessing models values. This may simplify future use of the models and reduce the impact of different storage and interpolation methods on the flux values. It should be also taken to the account, that the methods currently used in the NASA models, were developed 20 years ago, and modern computers can easily handle much more extensive calculations and finer grids.

References

Cosmos Model-82: 1983, Institue of Nuclear Physics, Moscow State University, Moscow

Daly, E.J., Evans, H.D.R.: 1993, *Problems in Radiation Environment Models at Low Altitudes*, Memorandum ESA/ESTEC/WMA/93

Gaffey, J.D.Jr., Bilitza, D.: 1994, *NASA/National Space Science Data Center Trapped Radiation Models*. Journal of Spacecraft and Rockets, **31**, 172–176

Getselev, I.V., Gusev, A.N., Darchieva, L.A., Kabashova, N.A., Morozova, T.I., Pavlov, A.V., Panasyuk, M.I., Pugacheva, G.I., Rejzman, S.Ya., Savun, O.I., Sosnovets, E.N., Tverskaya, N.V., Timofeyev, G.A., Yushkov, B.I.: 1991, *Model of Spatial-Energetic Distribution of Charged Particles (Protons and Electrons) Fluxes in the Earth's Radiation Belts*, INP MSU Preprint MGU-91-37/241, (in Russian)

Goriainov, M.F., Dronov, A.V., Kovtykh, A.S., Sosnovets, E.N.: 1983, *Spatial, Spectral and Anglular Structure of low-Altitude 30–210 kEV Electron Fluxes during Magnetically Quiet Time*, Kosmicheskie Islledovaniya, **21**, 609–618 (in Russian), translated in Cosmic Research, **21**, 494–500

GOST 25645-138.86 and 139.86: 1986 - *USSR State Standart on Earth's Radiation Belts Proton end Electron Fluxes*, Moscow (in Russian)

Grafodatsky, O.S., Islayev, Sh.N., Panasyuk, M.I., et.al.: 1989, *Magnetospheric Plasma Fluxes Registration on Board of GORISONT Satellite*, Issledovaanya po geomagnetismu, aeronomii, i physike Solntsa (Geomagnetism, Aeronomy and Solar Physics Studies), Issue 86, 99–130 (in Russian)

Heynderickx, D., Lemaire, J., Daly, E.J. :1994.*Historical Review of the Different Procedures Used to Compute the L-Parameter* submitted to J. of Nuclear Tracks and Radiation Measurements

McIlwain, C.E.: 1961, *Coordinates for Mapping the Distribution of Magnetically Trapped Protons* J. Geophys. Res. **66**, 3681–3691

Savun, O.I., Yushkov, B.Yu.: 1985, *Modeling of Charged Particles Fluxes along the Trajectories of Spacecrafts in the Earth's Radiation Belts*, Vestnik Moscovskogo Universiteta, seriya Physica i Asronomiya (Moscow University Courier, Physics

and Astronomy Series), **26**, 3 (in Russian)

Sawyer, D.M., Vette, J.I.: 1976, *AP-8 Trapped Proton Environment for Solar Maximum and Solar Minimum*, NSSDC/WDC-A-R&S 76-06

Teague, M.J., Stein, J., Vette, J.I.: 1975 *The Use of the Inner Zone Electron Model AE-5 and Associated Computer Programs*, NSSDC/WDC-A-&S 72-11

Vette, J.I.: 1977, *A Comparison of Trapped Proton Models AP8MIN and AP8MAX with Their Compressed Versions AP8MIC and AP8MAC*, NSSDC/WDC-A-R&S File No 13489

Vette, J.I.: 1991a, *The AE-8 Trapped Electron Environment*, NSSDC/WDC-A-R&S 91-24

Vette, J.I.: 1991b, *The NASA/National Space Science Data Center Trapped Radiation Environment Model Program*, NSSDC/WDC-A-R&S 91-29

Vlasova, N.A., Knyasev, B.N., Kovtykh, A.S., Kozlov, A.G., Panasyuk, M.I., Reyzman, S.Ya., Sosnovets, E.N.: 1984, *Protons with E ¿ 30 keV at Low Heights near Geomagnetic Equator during a Magnetically Quiet Time*, Kosmicheskie Islledovaniya, **22**, 53–66 (in Russian), translated in Cosmic Research, **22**, 46–58

Volkov, I.B., Dronov, A.B., Kratenko, Yu.P. et.al.: 1985, *Outer Electron Belt Dynamics according Simaltenious Measurements on Board of INTERCOSMOS-19 and COSMOS-900 Satellites*, Kosmicheskiye Islledovaniya (Cosmic Researches), **23**, 642–646 (in Russian)

Williams, D.J., Frank, C.A.: 1984, *Intense low energy ion populations at low equatorial altitudes*, J. Geophys. Res. **89**, 3903–3911